

Functional Convergence of Response Properties in the Auditory Thalamocortical System

Lee M. Miller,^{1,2,4,5} Monty A. Escabi,³
Heather L. Read,¹ and Christoph E. Schreiner^{1,2}

¹W.M. Keck Center for Integrative Neuroscience

²UCSF/UCB Bioengineering Group

University of California Medical Center
San Francisco, California 94143

³Electrical and Computer Engineering,
Bioengineering

University of Connecticut
Storrs, Connecticut 06269

Summary

One of the brain's fundamental tasks is to construct and transform representations of an animal's environment, yet few studies describe how individual neurons accomplish this. Our results from correlated pairs in the auditory thalamocortical system show that cortical excitatory receptive field regions can be directly inherited from thalamus, constructed from smaller inputs, and assembled by the cooperative activity of neuronal ensembles. The prevalence of functional thalamocortical connectivity is strictly governed by tonotopy, but connection strength is not. Finally, spectral and temporal modulation preferences in cortex may differ dramatically from the thalamic input. Our observations reveal a radical reconstruction of response properties from auditory thalamus to cortex, and illustrate how some properties are propagated with great fidelity while others are significantly transformed or generated intracortically.

Introduction

Sensory processing in the thalamocortical system has endured continual investigation since the earliest days of single-cell neurophysiology (Adrian, 1941). The most straightforward studies of thalamocortical function develop mechanistic models by comparing receptive fields from these anatomically subsequent stations (Hubel and Wiesel, 1962; Kyriazi and Simons, 1993). Others use more sophisticated methods, such as removing cortical influence to reveal only the thalamic contribution to cortical receptive fields (Chapman et al., 1991; Chung and Ferster, 1998). How the neurons construct and modify these response properties, however, has remained largely a matter of inference. Only a few studies have directly addressed the transformation of response properties between individual cells in the thalamus and cerebral cortex (Creutzfeldt et al., 1980; Tanaka, 1983; Swadlow, 1995; Reid and Alonso, 1995; Johnson and Alloway, 1996; Alonso et al., 2001).

The auditory system presents a unique challenge. In contrast to the visual thalamocortical system, which

shows the distinct transformation from center-surround to simple cell responses, auditory thalamic and cortical receptive fields are remarkably similar. Except for the well-known temporal slowing (Creutzfeldt et al., 1980), no fundamental response properties have been demonstrated to differ systematically across the lemniscal auditory thalamocortical synapse (Clarey et al., 1994). Nevertheless, thalamocortical anatomy would allow for massive functional convergence and divergence. Individual thalamic axons can ramify to span up to 7 mm of cortical space (de Venecia and McMullen, 1994; Cetas et al., 1999), and a single cortical locus can receive thalamic input from large regions in thalamus (Andersen et al., 1980; Middlebrooks and Zook, 1983; Brandner and Redies, 1990; H.L. Read et al., 1999, *Assoc. Res. Otolaryngol.*, abstract; Huang and Winer, 2000). It thus remains unclear what functional properties are being transformed across the auditory thalamocortical synapse. This study addresses the basic rules whereby auditory cortical receptive fields are constructed from their thalamic inputs.

We propose a heuristic framework of functional thalamocortical convergence types, then investigate several detailed aspects of the transformation, including: the spectral and temporal specificity of inputs to cortical cells, the complementary roles of excitatory and inhibitory receptive field subregions, and the thalamocortical transfer of spectral and temporal modulation properties. Recordings were made simultaneously from pairs of single units in the ventral medial geniculate body (MGBv) and its target layers in primary auditory cortex (AI) in the ketamine-anesthetized cat. Spectrotemporal receptive fields (STRFs) and spike train cross-correlations enabled us to evaluate the quality, strength, and specificity of functional thalamocortical convergence.

Results

Action potential trains from all thalamocortical pairs were cross-correlated. Functionally connected pairs ($n = 29$, from a total 741) of single units were chosen by the monosynaptic-like peaks in their correlograms, using strict criteria under both spontaneous and stimulus-driven conditions (see Experimental Procedures). Spectrotemporal receptive field properties were derived for each unit with reverse-correlation of a noise-like stimulus, the dynamic ripple. An STRF is the average spectrotemporal stimulus envelope immediately preceding an action potential. It shows positive regions in time and frequency where stimulus energy tends to increase firing rate, and negative regions where it decreases firing rate, relative to the mean.

Functional Convergence Types

The theoretically possible range of functional convergence can be heuristically characterized with three extremes: inheritance, constructive convergence, and en-

⁴Correspondence: lmill@socrates.berkeley.edu

⁵Present address: 3210 Tolman Hall, #1650, Department of Psychology, University of California, Berkeley, California, 94720.

Types of functional convergence

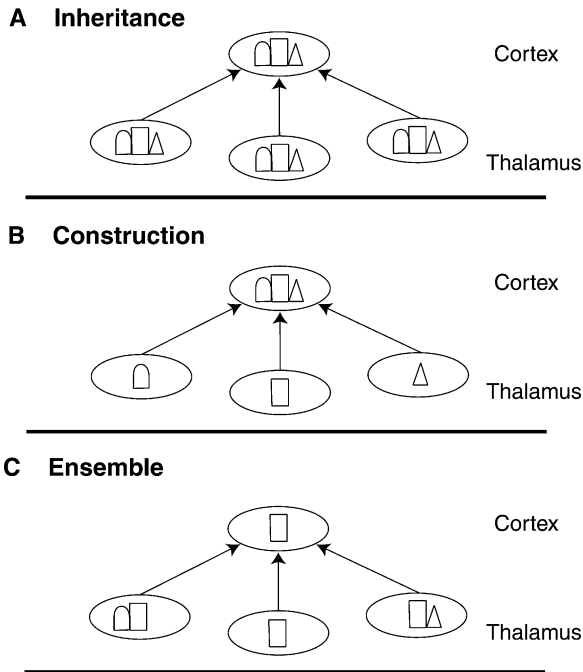


Figure 1. Heuristic Illustration of the Possible Extremes of Functional Thalamocortical Convergence

Shapes within the ellipses represent different spectrotemporal receptive field features. (A) The simplest case is inheritance, where a cortical cell's receptive field is determined by functionally identical thalamic inputs. (B) In constructive convergence, a cortical cell's receptive field is a composite of many smaller (in spatiotemporal extent) thalamic inputs. (C) In ensemble convergence, the thalamic inputs have some receptive field properties that are not shared by the cortical target cell. This requires an ensemble of other inputs either to amplify the features that are ultimately represented by the cortical cell, or to suppress the features that are not.

semble convergence (Figure 1). These extremes are not intended to be categorical: a given thalamocortical connection need not fall neatly into any one of these three. Nor do we expect a cortical receptive field to be made up of only one extreme convergence type. The three types illustrated simply delimit the possible range of functional convergence. For instance, inheritance (Figure 1A), the simplest case, occurs if a cortical cell's receptive field is completely determined by functionally identical thalamic inputs. Constructive convergence (Figure 1B) builds the cortical receptive field by integrating a number of thalamic inputs with smaller receptive fields, in frequency and/or time. This convergence-by-union is a variant of the Hubel-Wiesel model (Hubel and Wiesel, 1962; Tanaka, 1983; Reid and Alonso, 1995). Conversely, in ensemble convergence (Figure 1C), the thalamic inputs extend beyond the spectrotemporal borders of the resultant cortical receptive field. This convergence-by-intersection logically requires the participation of an ensemble of cells, cooperating either to amplify the receptive field regions that are ultimately represented in cortex, or to suppress regions that are not.

Representative functionally connected thalamocorti-

cal pairs are shown in Figure 2. In Figures 2A–2C, the excitatory peak in the thalamic STRF is in almost perfect register with that of the cortical cell. For assessing overlap (Figure 2C, contours), the thalamic STRF has been shifted in time by the peak correlogram delay, i.e., the expected travel and synaptic delay between the cells. The high similarity of STRFs suggests that a cortical unit could inherit its main excitatory region from functionally identical thalamic cells. Mixed constructive/ensemble convergence is shown in Figures 2D–2F, where a smaller, partially overlapping thalamic receptive field is integrated into a larger cortical receptive field. This emphasizes that convergence types in Figure 1 are not strictly categorical: the thalamic input not only participates in construction but also in ensemble convergence insofar as its excitatory region extends to frequencies beyond those of the cortical cell. Here, the nonoverlapping thalamic region appears to be an extension of the primary cortical excitatory region, and therefore may contribute to the subthreshold flanks of the cortical peak. Strong ensemble convergence appears in Figures 2G–2I, where a thalamic unit with large receptive field converges onto a cortical cell whose receptive field clearly composes only a subset of the thalamic input. Other functionally diverse inputs must cooperate to strengthen the region of overlap, elevating it above some threshold, or to suppress the nonoverlapping region. There is also an area of mismatch in this example, where strong thalamic excitation coincides with strong cortical inhibition. Evidently a large overlap of opposing features, at least with the further excitatory-excitatory match, need not preclude significant functional connectivity.

Rather than force each thalamocortical pair into one of the three functional convergence types, Figure 3 parses each pair along two continua: cortical coverage and thalamic overlap. Cortical coverage is the proportion of the cortical receptive field peak covered by that of the thalamus, where peaks are circumscribed by contours as in Figures 2C, 2F, and 2I ($1/e$ of maximum amplitude). Thalamic overlap is the proportion of the thalamic receptive field peak that overlaps that of the cortex. High cortical coverage and high thalamic overlap occur when the thalamic and cortical receptive fields are nearly identical, as for inheritance. Low cortical coverage but high thalamic overlap occurs when a small thalamic receptive field is completely subsumed by the cortical one, as in constructive convergence. Finally, low thalamic overlap with varying degrees of cortical coverage indicates ensemble convergence, when the thalamic input possesses receptive field regions that are not ultimately shared by the cortical cell. The paradigmatic receptive field relationships for these general ranges are indicated in Figure 3 (schematic insets). Functional thalamocortical pairs fill the entire domain of thalamic overlap and cortical coverage, demonstrating that the transformation of receptive fields utilizes all possible types of convergence.

Spectrotemporal Specificity

The spectrotemporal specificity of thalamocortical connections is addressed only indirectly by the metrics of Figure 3. To compare the pairwise specificity directly,

the thalamic inputs were normalized relative to their cortical targets. For Figure 4, the excitatory peak of each cortical target has been stretched in frequency and in time to match an arbitrary standard, which is plotted as a light gray circle (Figure 4A) with bandwidth and duration equal to one. Each thalamic input was then stretched by the same amount as its target, shifted by the correlogram peak delay, and plotted as a contour on the standardized axes. Such normalization maintains the relative thalamocortical overlap in frequency and time, allowing direct comparison across all pairs. Nearly all thalamic inputs show significant overlap with their cortical targets. The STRF energies within the contours, moreover, may be summed across time to give the distribution in relative frequency of the thalamic inputs (Figure 4B). Most (72%) of the energy falls within one normalized cortical bandwidth. Likewise, when the energies are summed across frequency, giving the distribution in relative timing of the thalamic inputs (Figure 4C), most (80%) of the input energy falls within one normalized cortical duration. Although our cross correlation criteria favor cell pairs that tend to fire in close temporal proximity, they do not require that all or most thalamic STRF energy should fall within a single cortical duration; cooperation with other inputs could easily bias the relative efficacy of thalamic spikes with a certain range of latencies, such that the STRF overlap in time could be marginal. Thus, thalamic input is highly specific in both relative frequency and relative time. On average, the inputs contribute very little excitatory energy outside the spectrotemporal extent of their cortical targets.

Another measure of frequency convergence is the best frequency difference between members of a functional pair. Figure 5A compares the differences of the thalamic best frequencies to those of their cortical targets (mean difference 0.077 octaves). If the best frequency difference exceeds about one quarter of an octave, functional thalamocortical connections disappear. Figure 5B shows the difference in the margins of the receptive field peaks (i.e., the edges on the frequency side farthest from the cortical best frequency) in octaves relative to the cortical best frequency. While this measure necessarily spans a larger frequency range, functional connections are still limited to about 1/3 octave.

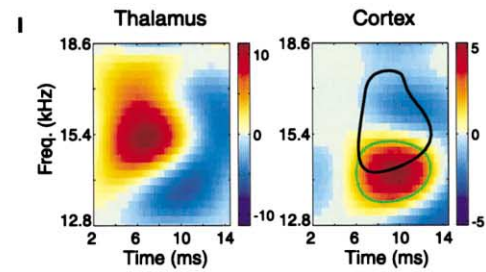
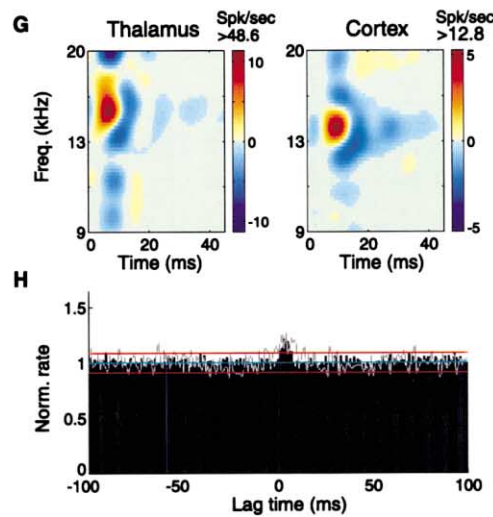
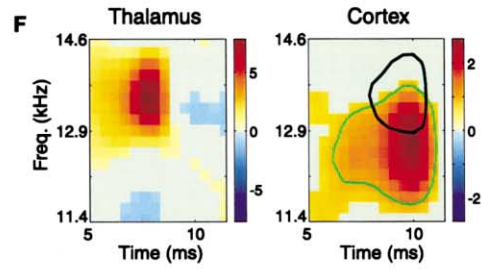
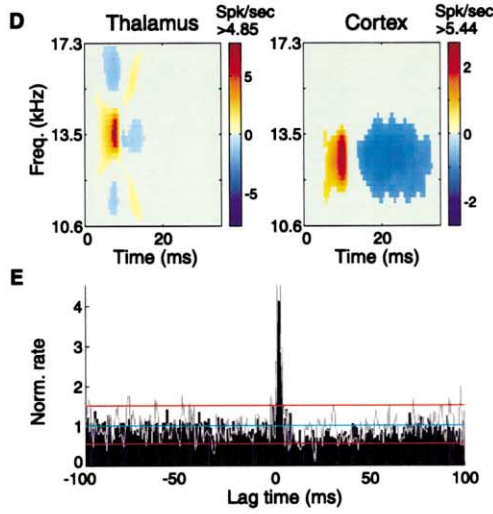
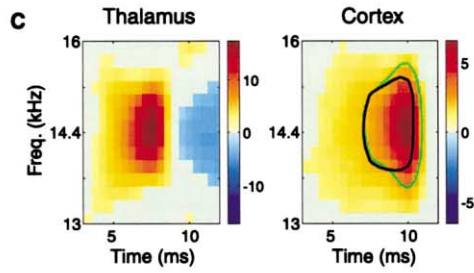
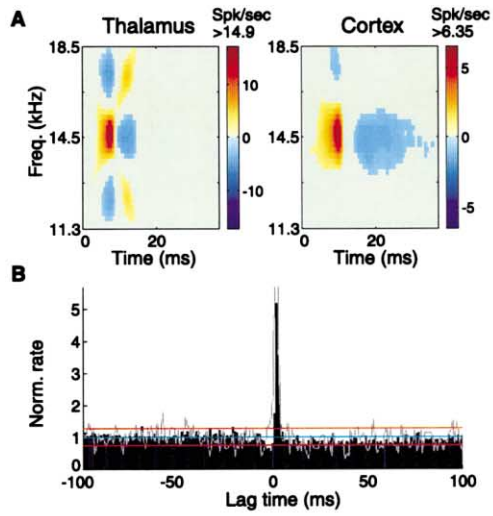
By considering the STRF differences between all recorded thalamocortical pairs, including the uncorrelated ones, we can determine how the prevalence of functional connectivity depends on receptive field similarity. The best frequency differences for all thalamocortical pairs reveals a sampling bias toward small differences (Figure 6A). On the basis of previous work (Creutzfeldt et al., 1980), we deliberately targeted pairs with small best frequency difference as they are most likely to be functionally connected. Although biased, our sample is continuous to differences greater than one octave. The highest proportion of correlated pairs has the smallest best frequency difference (Figure 6B). Interestingly, while the prevalence of functional correlation depends on frequency difference, the strength of the correlation does not (mean strength 0.045, median 0.026) (Figure 6C). A similar result emerges when we compare the entire STRFs, using a correlation coefficient called the similarity index (DeAngelis et al., 1999). In other modalities, the similarity index is typically used to capture only

spatial stimulus attributes. Our index instead considers the joint spectrotemporal response preferences for both neurons. It is thus a very strict measure of shared response properties; consequently, the population of all recorded pairs is biased toward low similarity indices (Figure 6D). Despite its sophistication, however, similarity index tends to be associated with the simpler measure of best frequency difference (corr. coef. = -0.69 , $p < 0.001$ for functionally connected pairs; -0.39 , $p < 0.001$ for all pairs). The prevalence of functionally connected pairs increases systematically with greater overall STRF similarity (Figure 6E). Nonetheless, as with best frequency alone, the strength of correlation does not depend on similarity index (Figure 6F).

Modulation and Inhibitory Properties

The spectrotemporal convergence described in Figures 3–6 is largely determined by a characteristic and ubiquitous lemniscal auditory receptive field feature, a main excitatory peak. Many response properties, however, depend not only on the excitatory region but on its relation to neighboring inhibitory regions. Two such response properties that are important for processing complex sounds are temporal and spectral modulation preferences. Best temporal modulation measures a neuron's preferred rate for energy in the stimulus to fluctuate in time. It is analogous to the speed of moving visual gratings. Best spectral modulation is a neuron's preferred size for spectral envelope contours. It is analogous to the spatial frequency of visual gratings.

With the dynamic ripple stimulus, modulation preferences are derived through a two-dimensional Fourier transform of the STRF. This yields a preferred value for temporal (in Hz) and spectral (in cycles per octave) modulations. In Figure 7A, the preferred temporal modulations for each pair are connected by lines. Temporal modulation preferences in cortex are slower than in thalamus (mean thalamus 44.3 Hz, cortex 27.5 Hz; median thalamus 48.2 Hz, cortex 21.5 Hz; paired-sample t test, $p = 0.0067$). While such slowing may be expected, it is notable that temporal modulation preferences in thalamus and cortex are not correlated by rank (Spearman rank correlation, $p > 0.2$): thalamic cells preferring the fastest modulations do not project preferentially to cortical cells preferring the fastest modulations, nor do slow thalamic cells project only to slow cortical cells. Many pairs including the examples from Figure 2 are evidently rank correlated, but given our entire sample, one is unable to predict cortical temporal preference from its thalamic input. Spectral modulation preferences (Figure 7B) show similar trends. Cortical neurons prefer significantly lower (broader) spectral modulation preferences than thalamic cells (mean thalamus 1.27 cyc/oct, cortex 0.49 cyc/oct; median thalamus 1.47 cyc/oct, cortex 0.18 cyc/oct; paired-sample t test $p < 0.001$). As with temporal modulations, spectral modulation preferences lack a ranked order (Spearman rank correlation, $p > 0.2$): thalamic cells preferring broad spectral envelopes have no privileged influence on cortical cells preferring broad envelopes, and narrow-preferring thalamic cells are not necessarily linked to narrow cortical cells. Thus, in contrast to the construction of first-order spectral and temporal envelope preferences for excitatory stimuli (Figure



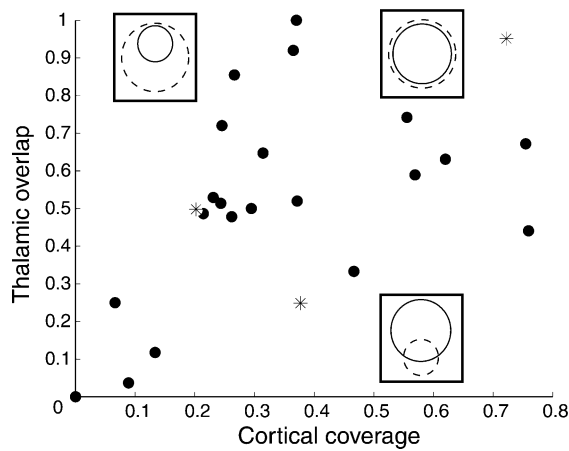


Figure 3. Distribution of Thalamocortical Convergence Types
Types of functional convergence for the main excitatory peak are parsed along two dimensions: cortical coverage and thalamic overlap. Cortical coverage is the proportion of the cortical receptive field peak covered by that of the thalamic input. Thalamic overlap is the proportion of the thalamic receptive field peak overlapping that of the cortex. Thus, high cortical coverage and thalamic overlap indicate inheritance; low cortical coverage but high thalamic overlap indicates constructive convergence; and low thalamic overlap with varying degrees of cortical coverage characterizes ensemble convergence. The schematic insets represent paradigmatic receptive field relationships for a given region of the plot, where dotted lines (---) represent the cortical, and solid lines (—) the thalamic receptive fields. Thalamocortical pairs from Figure 2 are represented by stars (*).

4), modulation preferences in both time and frequency are significantly transformed from thalamus to cortex.

Modulation properties depend essentially on the relationship between excitatory and inhibitory receptive field regions. The virtual absence of their propagation from thalamus to cortex, coupled with excitatory-inhibitory thalamic-cortical mismatches (Figure 2I), suggests that inhibitory receptive field features of thalamic neurons are far less important in the thalamocortical transformation. As a test of this hypothesis, similarity indices were calculated for each STRF pair. One index was computed only for excitatory thalamic features and another only for inhibitory thalamic features, relative to the cortical receptive field. The average similarity indices for

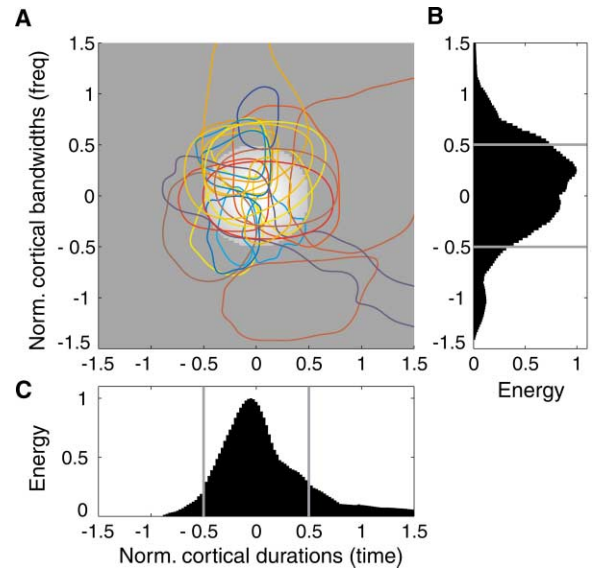


Figure 4. Summary of Normalized Thalamic Receptive Field Inputs
(A) An idealized cortical excitatory peak is depicted as a light gray circle. Contours outline the thalamic inputs, each normalized to its own cortical target. Contour color indicates thalamocortical correlation strength under the stimulus-driven condition (mean .045), with cool colors low and warm colors high values. (B) Peak energies of the thalamic inputs, summed across time. Most (72%) of the energy falls within one normalized cortical bandwidth (gray bars). (C) Peak energies of the thalamic inputs, summed across frequency. Most (80%) of the energy falls within one normalized cortical duration (gray bars).

excitatory input features (0.328 ± 0.18 , mean \pm SD) and inhibitory input features (0.123 ± 0.13 , mean \pm SD) differ significantly (paired-sample t test, $p < 0.001$). Excitatory receptive field features thus play a larger role than inhibitory features in functional thalamocortical connectivity.

Discussion

Functional Convergence Types

Our observations on the specificity and complexity of functional thalamocortical convergence in the auditory system have several implications for neural processing.

Figure 2. Representative Examples of Functionally Connected Thalamocortical Pairs

(A–C) Inheritance. (A) Spectrotemporal receptive fields (STRFs) for the thalamic and cortical cell (similarity index = 0.67). The STRFs are depicted with time-preceding-spike on the abscissa, and frequency on the ordinate. Warm and cool colors indicate an excitatory or inhibitory effect, respectively, that the stimulus induced in a particular spectrotemporal region. The values on the colorbar are thus differential rates, in spikes/s, relative to the mean rate. (B) Cross correlograms between the two units, normalized to firing rate. The bar plot is the cross correlogram under the ripple-driven condition, and the line plot (truncated for clarity) is under the spontaneous condition. The brief, short-latency peak, with cortical spike lagging thalamic (2 ms), is indicative of a monosynaptic-like functional connection (correlation strength = .082). The cyan line is the mean, and the red lines are the 99% confidence intervals for the stimulus-driven correlogram, under an assumption of independent, Poisson spike trains. (C) Expanded views of the excitatory peaks of the STRFs in (A). Superimposed on the cortical STRF are contours circumscribing the high-energy region of the cortical (green) and thalamic (black) STRFs (see Experimental Procedures). The thalamic contour has been shifted in time by the peak correlogram delay. In this case, the cortical cell appears to inherit its excitatory features from the thalamic input.

(D–F) Mixed constructive/ensemble convergence. (D) STRFs (similarity index = 0.43). (E) Thalamocortical cross correlograms (2 ms peak lag, correlation strength = .029). (F) Expanded views of the excitatory peaks. In this case, a thalamic cell with smaller receptive field helps construct a larger, composite cortical STRF. This example emphasizes that the convergence types schematized in Figure 1 are not, in fact, categorical.

(G–I) Ensemble convergence. (G) STRFs (similarity index = 0.29). (H) Thalamocortical cross correlograms (3 ms peak lag, correlation strength = .037). (I) Expanded views of the excitatory peaks. In this case, a thalamic cell with much larger excitatory receptive field is pared down to contribute to a smaller cortical STRF. This logically demands the participation of an ensemble of other inputs, acting in concert.

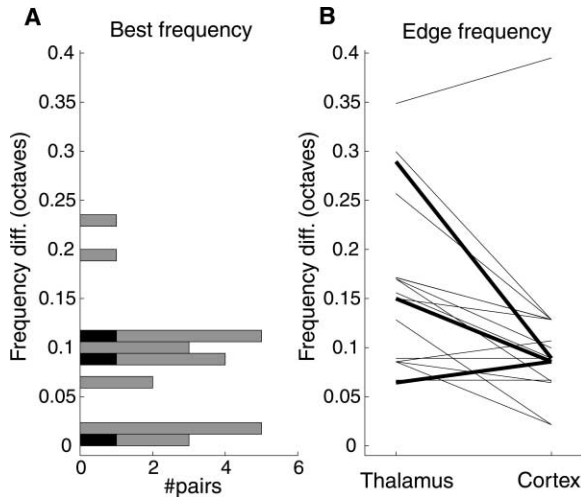


Figure 5. Degree of Thalamocortical Convergence in Octaves
(A) The difference in thalamic versus cortical best frequencies (absolute value) is summarized in a histogram (mean difference 0.077 octaves). Black bars are thalamocortical pairs from Figure 2. If the difference in best frequencies is greater than about 1/4 octave, functional connections are not observed. (B) For each thalamocortical pair, the frequencies at the far edges of the excitatory receptive fields, relative to cortical best frequency, are connected by a line. Very little convergence is observed for edges greater than 1/3 octave from the cortical best frequency. Due to the frequency sampling (~40/octave), several values from different pairs are so similar as to be indistinguishable. Thick lines are pairs from Figure 2.

Convergence types fill the possible space delimited by the three extremes of inheritance, construction, and ensemble convergence. Such variety is lacking in the visual system, where most thalamocortical connections respect a Hubel-Weisel type of constructive convergence model (Hubel and Wiesel, 1962; Tanaka, 1983; Reid and Alonso, 1995). While a given auditory cortical cell's receptive field may arise through any combination of functional convergence types, the extremes are nevertheless illustrative since each supports an operation the brain must perform upon sensory representations. Inheritance, where the cortical cell's receptive field is largely determined by functionally identical thalamic input, would preserve information for downstream processing. Constructive convergence would create selectivity for composite features, such as visual oriented lines or auditory formant combinations. Ensemble convergence, by requiring cooperative inputs to amplify some parts of the input and/or suppress others, would support feature selectivity of a more exacting nature than at the previous processing station. Admittedly, since no thalamocortical connections are of a one-to-one nature, all convergence is some type of "ensemble" convergence. Our analysis, however, explores the constraints on and distribution of conceptually distinct convergence types.

Spectrotemporal Specificity

Thalamocortical specificity is highly focal in both spectral and temporal domains, with most of the excitatory input energy falling within the cortical receptive field. This strong concentration of energy occurs despite the prevalence of ensemble convergence, which would tend

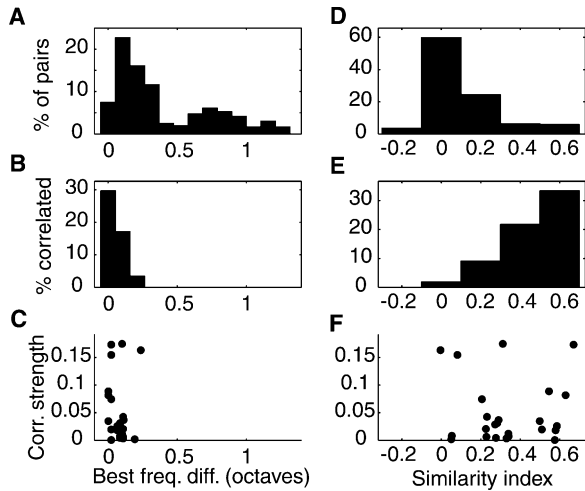


Figure 6. Prevalence but Not Strength of Functional Connectivity Depends on Best Frequency Difference and Similarity Index
(A) A histogram of all recorded thalamocortical pairs reveals a sampling bias toward pairs with small best frequency difference but extends well beyond one-octave separation. (B) The proportion of recorded pairs that are functionally correlated depends strongly on the best frequency difference, with the greatest proportion having the least difference. (C) The strength of correlation for functionally connected thalamocortical pairs does not depend on best frequency difference. (D) Our population of all recorded thalamocortical pairs is biased toward low, positive similarity indices. (E) The proportion of recorded pairs that are functionally correlated depends strongly on the overall STRF similarity. (F) The strength of correlation for functionally connected thalamocortical pairs does not depend on STRF similarity.

to smear the input energy across a wider spectrotemporal region. Such highly specific coupling occurs between the lateral geniculate and primary visual cortex (Tanaka, 1983; Reid and Alonso, 1995; Alonso et al., 2001), suggesting that functional convergence in any thalamocortical modality is highly accurate. In the auditory system, moreover, we show that physiological convergence is constrained to within approximately 1/3 octave, or a single critical band, the benchmark human psychophysical measure for cross-frequency integration (Scharf, 1970). Neural correlates of the critical band have also been demonstrated in the inferior colliculus, the main input structure to the auditory thalamus (Schreiner and Langner, 1997).

The prevalence of functional connectivity is strictly determined by tonotopy and overall thalamocortical receptive field similarity. Remarkably, up to thirty percent of recorded pairs with virtually the same best frequency (within 0.05 octaves) are functionally connected. Likewise, if the thalamic and cortical receptive fields have an extremely high similarity index, a large proportion are connected. These proportions match precisely those in the visual system for thalamic-cortical cell pairs with spatially overlapping receptive fields (Alonso et al., 2001). In the primary visual cortex, however, two-dimensional retinotopy is well preserved across the cortical sheet, whereas in the auditory system, each epithelial location (frequency) is represented across an entire band of cortex, many millimeters in length. Thalamic inputs are patchy and various response properties clus-

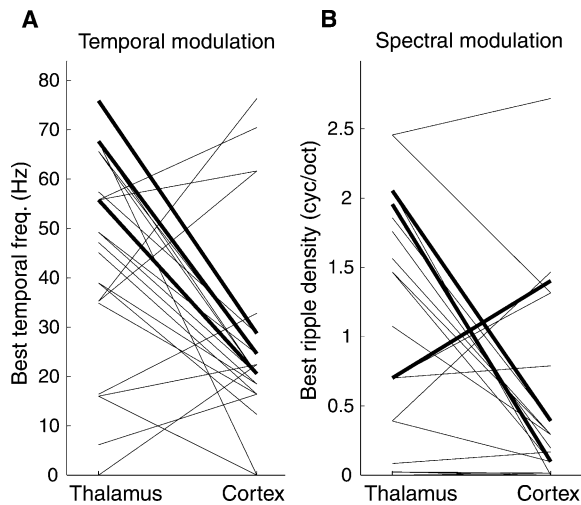


Figure 7. Convergence of Temporal and Spectral Modulation Preferences

(A) Temporal modulation preferences for each thalamocortical pair, in Hz, are connected by lines. Cortical cells tend to prefer slower modulations (mean thalamus 44.3 Hz, cortex 27.5 Hz; median thalamus 48.2 Hz, cortex 21.5 Hz; paired-sample *t* test, $p = 0.0067$). There is no rank correlation among the pairs; that is, slow (fast) thalamic cells do not tend to project to slow (fast) cortical cells (Spearman rank correlation, $p > 0.2$). (B) Spectral modulation preferences for each thalamocortical pair, in ripple cycles per octave, are connected by lines. There is a significant trend toward broader, or wider-band preferences in cortex (mean thalamus 1.27 Hz, cortex 0.49 Hz; median thalamus 1.47 Hz, cortex 0.18 Hz; paired-sample *t* test $p < 0.001$). As with temporal modulations, there is no rank correlation among the pairs: broad (narrow) thalamic cells do not project preferentially to broad (narrow) cortical cells (Spearman rank correlation, $p > 0.2$). Thick lines are pairs from Figure 2.

ter in a modular fashion along such isofrequency contours (for review, see Schreiner et al., 2000). While this report considers the most dominant response properties, other factors not addressed here may affect connectivity; it is therefore surprising that such a large percentage of auditory thalamocortical cell pairs are functionally connected. Our sampling biases reveal, however, that it is experimentally very difficult to find such pairs.

Although the prevalence of functional connectivity depends on receptive field similarity, the strength of connectivity does not. This result differs substantially from the visual system, where correlation strength is strictly constrained by receptive field overlap (Alonso et al., 2001). In the auditory system, strong functional connections occur not only between cells with well-matched receptive fields, as with the inheritance type of convergence. Equally powerful connections occur between cells with few receptive field features in common, as with ensemble convergence. Average connection strength is a rough guide to the number of thalamic inputs that drive a typical cortical target. Our mean connection strength of 0.045 suggests that 20–25 thalamic inputs are required to fully activate a cortical cell. Since our analysis does not consider cooperation among inputs, however, this value probably underestimates the actual numerical convergence (Reid and Alonso, 1995; Alonso et al., 2001). These approximations also ignore the fact

that many inputs onto a cortical cell in the thalamorecipient layers are of cortical origin.

Given the large range of convergence that thalamocortical anatomy would allow, the high degree of functional specificity raises the possibility that many nonfunctional or subthreshold synapses exist outside the bounds of physiologically identified convergence (Schroeder et al., 1995; Moore and Nelson, 1998; Feldman et al., 1999; Bringuier et al., 1999; Carandini and Ferster, 2000). Such a network could selectively integrate inputs with certain parameters, and thus may establish the basis of functional zones in primary auditory cortex (Schreiner et al., 2000). It would also constitute a coding system capable of great plasticity. If an otherwise uncommitted pool of neighboring, nonfunctional connections were subject to recruitment, then the network could support significant changes in response to neural damage or behaviorally relevant stimuli (Recanzone et al., 1993; Weinberger, 1995; Rajan and Irvine, 1998; Kilgard and Merzenich, 1998; Nicolelis et al., 1998; Jones and Pons, 1998). This plasticity, moreover, would be uncorrelated for spectrotemporal excitatory versus envelope modulation properties (Kilgard and Merzenich, 1998) since the thalamocortical transformation treats these factors independently.

Modulation and Inhibitory Properties

Modulation preferences are not well preserved from thalamus to cortex, even in a lower-valued but ranked order. This transformation differs from the visual system, where similarities in spatial modulation (on-off subregion size and relative position) and temporal modulation (impulse response) properties both influence the presence of monosynaptic connectivity (Alonso et al., 2001). Mechanistically, it reflects the fact that although excitatory receptive field properties are decisive in functional correlation, inhibitory features are not transmitted with great fidelity. The dichotomy implies that excitatory receptive field subregions of input-layer cortical cells are driven by direct thalamic input, while the inhibitory subregions, and thus modulation properties, are constructed or at least strengthened intracortically. That is, inhibitory subregions of cortical cells do not appear to come about through withdrawal of the solely excitatory thalamic input; rather, they likely come about through active inhibition from cortical interneurons. Evidence of such active excitatory/inhibitory (“push/pull”) circuitry has been observed in the visual and somatosensory systems (Ferster, 1988; Hirsch et al., 1998; Swadlow and Gusev, 2000; Ferster and Miller, 2000), but the imbalance may be more pronounced in the auditory system.

Functionally, temporal and spectral modulations are essential for discriminating complex auditory signals. In human speech for instance, spectral modulations distinguish vowels such as “eeh” and “ooh,” which differ in the spacing of their spectral peaks or formants. Temporal modulations distinguish consonants such as “buh” and “puh,” which differ in a quality called voice-onset-time. The fact that neural preferences for spectral and temporal modulations undergo a radical reorganization from thalamus to cortex suggests that the two stations may process modulations in different ways. The differences could take at least two forms: how modulations are coded or what range of modulations is represented. For

example, the maximum temporal modulation frequency represented by phase-locked neural activity decreases progressively from inferior colliculus to cortex. Some investigators provide evidence that high-frequency phase-locked responses in inferior colliculus are replaced in cortex by a topographic, rate-based neural code (Pantev et al., 1989; Langner et al., 1997; but see Fishman et al., 1998). Other studies emphasize the psychophysical salience of low (<20 Hz) temporal modulations instead (Drullman et al., 1994; Arai and Greenberg, 1998), thereby implying that the phase-locked preferences observed in cortex could be a specialization for this lower range. Our analysis only considered phase-locked responses to modulations, so we cannot address these questions directly. Nevertheless, the lack of preservation of modulation preferences from thalamus to cortex indicates that a distinct functional transformation takes place between the two stations.

Concluding Remarks

This investigation has considered only the robust, feed-forward convergence of neural response properties phase-locked to the stimulus envelope. Our selection criteria under both spontaneous and stimulus-driven conditions ensure that only robust functional correlations were studied. Since cross-correlation is a noisy measure, our dataset naturally favors the strongest connections. Weaker or labile functional connections may embody different convergence properties. Especially in the awake animal, dynamic state and corticofugal feedback may have powerful effects on the strength and quality of thalamic input to cortical receptive fields (Zhang and Suga, 1997; Fanselow and Nicolelis, 1999; Wörgötter and Eysel, 2000). Moreover, parallel non-lemniscal pathways may perform different operations than the primary lemniscal network (Ahissar et al., 2000). Finally, the STRFs used here are linear descriptors with respect to, and are necessarily phase-locked with, the spectrotemporal envelope. The high degree of functional specificity for excitatory receptive field features, however, makes it unlikely that even-order, phase-invariant nonlinearities significantly affect the transformation between these cell pairs.

This report describes what information is and, importantly, what information is not preserved in the auditory thalamocortical transformation. It illustrates how the brain realizes the varieties of functional convergence, whether by direct inheritance or with cooperative ensembles of inputs. Above all, it shows how a remarkable specificity of connections coexists with a fundamental reconstruction of receptive fields in cortex. We therefore not only address an essential gap in our knowledge of the auditory system, where no investigation of this type has ever been performed, but also illustrate its relevance to other modalities. By comparing our results with those in the visual and somatosensory systems, we can discriminate between processes specialized for a given modality and characteristics common to the general thalamocortical transformation.

Experimental Procedures

Electrophysiology

Some of the experimental methods have been reported previously (Miller and Schreiner, 2000). Young adult cats ($N = 4$) were anesthe-

tized with Nembutal (15–30 mg/kg) during the surgical procedure. After surgery, the animals were maintained in an unreflexive state with a continuous infusion of ketamine/diazepam (10 mg/kg ketamine, 0.5 mg/kg diazepam in lactated ringer's solution). All procedures were in strict accordance with the UCSF Committee for Animal Research and the guidelines of the Society for Neuroscience.

All recordings were made with the animal in a sound-shielded anechoic chamber (IAC, Bronx, NY), with stimuli delivered via a closed, binaural speaker system (diaphragms from Stax, Japan). Simultaneous extracellular recordings were made in the thalamorecipient layers (IIIb/IV) of the primary auditory cortex (AI) and in the ventral division of the medial geniculate body (MGBv). Electrodes were parylene-coated tungsten (Microprobe Inc., Potomac, MD) with impedances of 1–2 M Ω , or 3–5 M Ω tungsten electrodes plated with platinum black. One or two electrodes were placed in each station with hydraulic microdrives on mechanical manipulators (Narishige, Tokyo, Japan), mounted on a stereotaxic frame (David Kopf Instruments, Tujunga, CA) or on supplementary supports. Localization of thalamic electrodes, which were stereotaxically advanced along the vertical, was confirmed with Nissl stained sections; we did not distinguish between pars lateralis and pars ovoidea within the ventral division of the medial geniculate. Within the constraints described above, none of our results appeared to depend on cortical or thalamic electrode location. Spike trains were sorted offline with a Bayesian spike sorting algorithm (Lewicki, 1994). Each electrode location yielded an average of 1.9 well-isolated single units. Spontaneous neural activity (in silence) was recorded for about 35 min, and stimulus-driven activity for approximately 20 min.

Stimulus

The dynamic ripple stimulus (Schreiner and Calhoun, 1994; Kowalski et al., 1996; M.A. Escabí et al., 1998, Soc. Neurosci., abstract; Miller and Schreiner, 2000) is a temporally varying broadband sound composed of 230 sinusoidal carriers (500–20,000 Hz) with randomized phase. The magnitude of any carrier at any time is modulated by the spectrotemporal envelope, consisting of sinusoidal amplitude peaks ("ripples") on a logarithmic frequency axis which change through time. Two parameters define the envelope: the number of spectral peaks per octave, or ripple density, and the speed and direction of the peaks' change, or temporal frequency modulation. Both ripple density and temporal frequency modulation rate were varied randomly and independently during the 20 min, nonrepeating stimulus. Ripple density varied slowly (max. rate of change 1 Hz) between 0 and 4 cycles per octave; the temporal frequency modulation parameter varied between 0 and 100 Hz (max. rate of change 3 Hz). Both parameters were statistically independent and unbiased within those ranges. In one experiment, however, the temporal modulation spectrum decayed slightly; all evidence of this mild bias was readily abolished while thresholding the STRFs (see Analysis). Maximum modulation depth of the spectrotemporal envelope was 45 dB. Mean intensity was set approximately 20–30 dB above the neurons' thresholds to best frequency pure tones of 50 ms duration and 5 ms linear rise/fall envelope; thalamic and cortical thresholds were typically very similar.

Analysis

Data analysis was carried out in MATLAB (Mathworks Inc., Natick, MA). Spike trains were cross-correlated (Perkel et al., 1967) with 1 ms bin width, and significant bins ($p < 0.01$) were determined with respect to an independent, Poisson assumption. Functionally connected pairs of neurons ($n = 29$, from a total 741) were chosen by a strict set of criteria. Most pairs, including those in Figure 2, showed a maximum and significant correlogram peak within 1–5 ms lag time, thalamus leading cortex, under both spontaneous and stimulus-driven conditions. It is important to use spontaneous activity when possible, as it indicates functional connectivity when the auditory system is at rest, in terms of representing stimuli. Thus, by requiring monosynaptic-like peaks under both spontaneous and driven conditions, we select particularly stable functional connections. There are, however, two potential difficulties with using spontaneous activity. The first is that a widespread, oscillatory state in the 7–14 Hz range may obscure fast correlation features (Eggermont, 1992; Cotillon et al., 2000; Miller and Schreiner, 2000). Therefore, if

thalamocortical oscillations were present under the spontaneous condition, as indicated by a significant peak in the power spectrum between 7–14 Hz, the correlogram was high-pass filtered above 25 Hz. This eliminates broad, unspecific correlation peaks and leaves intact the narrow, specific peaks that reflect direct functional connectivity. The significance level was then adjusted accordingly, and the 1–5 ms peak criterion applied. The second challenge in using spontaneous activity is that some neurons' spike rates are so low in silence that their correlograms are too noisy to show significant features. To avoid biasing our sample toward neurons with high spontaneous rates, we applied an additional, more conservative criterion. We looked more closely at recording locations where some pairs showed the significant, maximum 1–5 ms peak in both conditions, and considered thalamocortical pairs whose spontaneous correlograms' coefficient of variation exceeded one for the presumably featureless range of ± 300 –3000 ms. If those pairs also had a very fast (3 ms width at half-height), short-latency (1–5 ms lag) peak under the driven condition, they were included in the analysis ($n = 6$). Given intrinsic response variability to the dynamic ripple stimulus in thalamus and cortex, this criterion is strict enough that pairs with solely stimulus-driven correlations are rejected; with typical quasi-linear responses, the peak width is so brief that our maximum driving rate of 100 Hz is too slow to account for it. Thus in finding functionally connected pairs, we usually used both spontaneous and driven activity, and otherwise applied an even more stringent criterion to the driven activity to rule out solely stimulus-driven correlogram features. Two pairs were excluded from the analysis because either the cortical unit ($n = 1$) or the thalamic unit ($n = 1$) had an STRF too weak to characterize; all other units yielded robust STRFs with excitatory and inhibitory subfields. Finally, three pairs were excluded because the receptive field features extended beyond our frequency sampling range (500–20,000 Hz).

Strength of correlation was computed under driven conditions with the traditional measure of contribution (Levick et al., 1972). Contribution is the percentage of cortical spikes immediately preceded by a thalamic spike (1–10 ms lag), above that expected by chance. Intuitively, the contribution gives the proportion of the cortical cell's activity that is presumed to be caused by the thalamic unit.

For each neuron, the reverse correlation method was used to derive the spectrotemporal receptive field, or STRF, which is the average spectrotemporal stimulus envelope immediately preceding each spike (Aertsen and Johannesma, 1980; M.A. Escabí et al., 1998, *Soc. Neurosci.*, abstract; Klein et al., 2000). In this report, only STRFs derived from the typically dominant, contralateral ear were used. For display, the STRFs were thresholded to show significant regions ($p < 0.002$). High-energy peaks in the STRF were defined by contours at $1/e$ times the maximum value, which typically circumscribed approximately 90% of the peak energy. Best frequency was the location of the maximum STRF pixel. Modulation properties were derived by performing a two-dimensional Fourier transform of the STRF, giving a signal in the parameter space of temporal modulation rate versus spectral modulation rate, or ripple density.

Thalamic and cortical STRFs were compared with a similarity index (DeAngelis et al., 1999) related to a correlation coefficient. For functionally connected pairs, the thalamic STRF was shifted by the peak correlogram lag, an estimate of axonal and synaptic delay. For nonconnected pairs, the thalamic STRF was shifted by the mean delay for all connected pairs of 2.6 ms. The two significant STRFs were then treated as vectors rather than arrays in time and frequency. The similarity index is the inner product of the vectorized thalamic and cortical STRFs, divided by both of their vector norms. A vector norm is the square root of the inner product of a vector with itself. Therefore, STRFs that are similar in shape and sign have a similarity index near 1, those of similar shape but opposite sign have an index near -1 , and those that are orthogonal have an index of 0. Thalamocortical similarity indices were calculated with the entire thalamic STRF and with excitatory and inhibitory thalamic subregions separately. Since all thalamocortical connections are excitatory, inhibitory subregions would be most directly transmitted through a withdrawal of thalamic excitation. More circuitous routes of transmission are likely, but they entail sequential processing across additional intracortical synapses. Given typical interneuronal connection strengths, however, each additional synapse would result in a transmission loss of one or more orders of magnitude, and

sequential losses would be multiplicative. Consequently, we would not expect robust thalamocortical transmission of individual subfields at long or highly variable latencies. In assessing direct thalamocortical influences, therefore, the effect of the STRF time shift is equivalent for excitatory and inhibitory subfields and is given by the peak correlogram lag; the latency for an increase in excitation is the same as the latency for withdrawal.

Acknowledgments

This work was supported by the National Institutes of Health (DC-02260, NS34835), the National Science Foundation (NSF97203398), and the Whitaker Foundation. Thanks to M. Kvale for writing the spike-sorting software.

Received May 7, 2001; revised July 19, 2001.

References

- Adrian, E.D. (1941). Afferent discharges to the cerebral cortex from peripheral sense organs. *J. Physiol.* *100*, 159–191.
- Aertsen, A.M.H.J., and Johannesma, P.I.M. (1980). Spectro-temporal receptive fields of auditory neurons in the grassfrog. *Biol. Cyber.* *38*, 223–234.
- Ahissar, E., Sosnik, R., and Haidarliu, S. (2000). Transformation from temporal to rate coding in a somatosensory thalamocortical pathway. *Nature* *406*, 302–306.
- Alonso, J.M., Usrey, W.M., and Reid, R.C. (2001). Rules of connectivity between geniculate cells and simple cells in cat primary visual cortex. *J. Neurosci.* *21*, 4001–4015.
- Andersen, R.A., Knight, P.L., and Merzenich, M.M. (1980). The thalamocortical and corticothalamic connections of AI, AII, and the anterior auditory field (AAF) in the cat: evidence for two largely segregated systems of connections. *J. Comp. Neurol.* *194*, 663–701.
- Arai, T., and Greenberg, S. (1998). Speech intelligibility in the presence of cross-channel spectral asynchrony. In *Proceedings of the 1998 IEEE International Conference on Acoustics, Speech and Signal Processing*, Vol. 2. (New York: IEEE), pp.933–936.
- Brandner, S., and Riedes, H. (1990). The projection from medial geniculate to field AI in cat: organization in the isofrequency dimension. *J. Neurosci.* *10*, 50–61.
- Binguier, V., Chavane, F., Glaeser, L., and Frégnac, Y. (1999). Horizontal propagation of visual activity in the synaptic integration field of area 17 neurons. *Science* *283*, 695–699.
- Carandini, M., and Ferster, D. (2000). Membrane potential and firing rate in cat primary visual cortex. *J. Neurosci.* *20*, 470–484.
- Cetas, J.S., de Venecia, R.K., and McMullen, N.T. (1999). Thalamocortical afferents of Lorente de Nó: medial geniculate axons that project to primary auditory cortex have collateral branches to layer I. *Brain Res.* *830*, 203–208.
- Chapman, B., Zahs, K.R., and Stryker, M.P. (1991). Relation of cortical cell orientation selectivity to alignment of receptive fields of the geniculocortical afferents that arborize within a single orientation column in ferret visual cortex. *J. Neurosci.* *11*, 1347–1358.
- Chung, S., and Ferster, D. (1998). Strength and orientation tuning of the thalamic input to simple cells revealed by electrically evoked cortical suppression. *Neuron* *20*, 1177–1189.
- Clarey, J.C., Barone, P., and Imig, T.J. (1994). Physiology of thalamus and cortex. In *The Mammalian Auditory Pathway: Neurophysiology*, A.N. Popper and R.R. Fay, eds. (New York: Springer-Verlag), pp. 232–334.
- Cotillon, N., Nafati, M., and Edeline, J.M. (2000). Characteristics of reliable tone-evoked oscillations in the rat thalamo-cortical auditory system. *Hear. Res.* *142*, 113–130.
- Creutzfeldt, O., Hellweg, F.C., and Schreiner, C.E. (1980). Thalamocortical transformation of responses to complex auditory stimuli. *Exp. Brain Res.* *39*, 87–104.
- DeAngelis, G.C., Ghose, G.M., Ohzawa, I., and Freeman, R.D. (1999). Functional micro-organization of primary visual cortex: receptive field analysis of nearby neurons. *J. Neurosci.* *19*, 4046–4064.

- de Venecia, R.K., and McMullen, N.T. (1994). Single thalamocortical axons diverge to multiple patches in neonatal auditory cortex. *Brain Res. Dev. Brain Res.* 81, 135–142.
- Drullman, R., Festen, J.M., and Plomp, R. (1994). Effect of temporal envelope smearing on speech reception. *J. Acoust. Soc. Am.* 95, 1053–1064.
- Eggermont, J.J. (1992). Stimulus induced and spontaneous rhythmic firing of single units in cat primary auditory cortex. *Hear. Res.* 61, 1–11.
- Fanselow, E.E., and Nicolelis, M.A. (1999). Behavioral modulation of tactile responses in the rat somatosensory system. *J. Neurosci.* 19, 7603–7616.
- Feldman, D.E., Nicoll, R.A., and Malenka, R.C. (1999). Synaptic plasticity at thalamocortical synapses in developing rat somatosensory cortex: LTP, LTD, and silent synapses. *J. Neurobiol.* 41, 92–101.
- Ferster, D. (1988). Spatially opponent excitation and inhibition in simple cells of the cat visual cortex. *J. Neurosci.* 8, 1172–1180.
- Ferster, D., and Miller, K.D. (2000). Neural mechanisms of orientation selectivity in the visual cortex. *Annu. Rev. Neurosci.* 23, 441–471.
- Fishman, Y.I., Reser, D.H., Arezzo, J.C., and Steinschneider, M. (1998). Pitch vs. spectral encoding of harmonic complex tones in primary auditory cortex of the awake monkey. *Brain Res.* 786, 18–30.
- Hirsch, J.A., Alonso, J.-M., Reid, R.C., and Martinez, L.M. (1998). Synaptic integration in striate cortical simple cells. *J. Neurosci.* 18, 9517–9528.
- Huang, C.L., and Winer, J.A. (2000). Auditory thalamocortical projections in the cat: laminar and areal patterns of input. *J. Comp. Neurol.* 427, 302–331.
- Hubel, D.H., and Wiesel, T.N. (1962). Receptive fields, binocular interaction and functional architecture in the cat's visual cortex. *J. Physiol. (Lond.)* 160, 106–154.
- Johnson, M.J., and Alloway, K.D. (1996). Cross-correlation analysis reveals laminar differences in thalamocortical interactions in the somatosensory system. *J. Neurophysiol.* 75, 1444–1457.
- Jones, E.G., and Pons, T.P. (1998). Thalamic and brainstem contributions to large-scale plasticity of primate somatosensory cortex. *Science* 282, 1121–1125.
- Kilgard, M.P., and Merzenich, M.M. (1998). Plasticity of temporal information processing in the primary auditory cortex. *Nat. Neurosci.* 1, 727–731.
- Klein, D.J., Depireux, D.A., Simon, J.Z., and Shamma, S.A. (2000). Robust spectrotemporal reverse correlation for the auditory system: optimizing stimulus design. *J. Comp. Neurosci.* 9, 85–111.
- Kowalski, N., Depireux, D.A., and Shamma, S.A. (1996). Analysis of dynamic spectra in ferret primary auditory cortex. I. Characteristics of single-unit responses to moving ripple spectra. *J. Neurophysiol.* 76, 3503–3523.
- Kyriazi, H.T., and Simons, D.J. (1993). Thalamocortical response transformations in simulated whisker barrels. *J. Neurosci.* 13, 1601–1615.
- Langner, G., Sams, M., Heil, P., and Schulze, H. (1997). Frequency and periodicity are represented in orthogonal maps in the human auditory cortex: evidence from magnetoencephalography. *J. Comp. Physiol. A. Sens. Neur. Behav. Physiol.* 181, 665–676.
- Levick, W.R., Cleland, B.G., and Dubin, M.W. (1972). Lateral geniculate neurons of cat: retinal inputs and physiology. *Invest. Ophthalmol.* 11, 302–311.
- Lewicki, M.S. (1994). Bayesian modeling and classification of neural signals. *Neural Comp.* 6, 1005–1030.
- Middlebrooks, J.C., and Zook, J.M. (1983). Intrinsic organization of the cat's medial geniculate body identified by projections to binaural response-specific bands in the primary auditory cortex. *J. Neurosci.* 3, 203–224.
- Miller, L.M., and Schreiner, C.E. (2000). Stimulus-based state control in the thalamocortical system. *J. Neurosci.* 20, 7011–7016.
- Moore, C.I., and Nelson, S.B. (1998). Spatio-temporal subthreshold receptive fields in the vibrissa representation of rat primary somatosensory cortex. *J. Neurophysiol.* 80, 2882–2892.
- Nicolelis, M.A., Katz, D., and Krupa, D.J. (1998). Potential circuit mechanisms underlying concurrent thalamic and cortical plasticity. *Rev. Neurosci.* 9, 213–224.
- Pantev, C., Hoke, M., Lütkenhöner, B., and Lehnertz, K. (1989). Tono-topographic organization of the auditory cortex: pitch versus frequency representation. *Science* 246, 486–488.
- Perkel, D.H., Gerstein, G.L., and Moore, G.P. (1967). Neuronal spike trains and stochastic point processes. II. Simultaneous spike trains. *Biophys. J.* 7, 419–440.
- Rajan, R., and Irvine, D.R. (1998). Neuronal responses across cortical field A1 in plasticity induced by peripheral auditory organ damage. *Audiol. Neurootol.* 3, 123–144.
- Recanzone, G.H., Schreiner, C.E., and Merzenich, M.M. (1993). Plasticity in the frequency representation of primary auditory cortex following discrimination training in adult owl monkeys. *J. Neurosci.* 13, 87–103.
- Reid, R.C., and Alonso, J.-M. (1995). Specificity of monosynaptic connections from thalamus to visual cortex. *Nature* 378, 281–284.
- Scharf, B. (1970). Critical bands. In *Foundations of Modern Auditory Theory*, Vol. 1, J.V. Tobias, ed. (New York: Academic Press), pp. 159–202.
- Schreiner, C.E., and Calhoun, B.M. (1994). Spectral envelope coding in cat primary auditory cortex: properties of ripple transfer functions. *Audit. Neurosci.* 1, 39–61.
- Schreiner, C.E., and Langner, G. (1997). Laminar fine structure of frequency organization in auditory midbrain. *Nature* 388, 383–386.
- Schreiner, C.E., Read, H.L., and Sutter, M.L. (2000). Modular organization of frequency integration in primary auditory cortex. *Annu. Rev. Neurosci.* 23, 501–529.
- Schroeder, C.E., Seto, S., Arezzo, J.C., and Garraghty, P.E. (1995). Electrophysiological evidence for overlapping dominant and latent inputs to somatosensory cortex in squirrel monkeys. *J. Neurophysiol.* 74, 722–732.
- Swadlow, H.A. (1995). Influence of VPM afferents on putative inhibitory interneurons in S1 of the awake rabbit: evidence from cross-correlation, microstimulation, and latencies to peripheral sensory stimulation. *J. Neurophysiol.* 73, 1584–1599.
- Swadlow, H.A., and Gusev, A.G. (2000). The influence of single VB thalamocortical impulses on barrel columns of rabbit somatosensory cortex. *J. Neurophysiol.* 83, 2802–2813.
- Tanaka, K. (1983). Cross-correlation analysis of geniculostriate neuronal relationships in cats. *J. Neurophysiol.* 49, 1303–1318.
- Weinberger, N.M. (1995). Dynamic regulation of receptive fields and maps in the adult sensory cortex. *Annu. Rev. Neurosci.* 18, 129–158.
- Wörgötter, F., and Eysel, U.T. (2000). Context, state and the receptive fields of striatal cortex cells. *Trends Neurosci.* 23, 497–503.
- Zhang, Y., and Suga, N. (1997). Corticofugal amplification of subcortical responses to single tone stimuli in the mustached bat. *J. Neurophysiol.* 78, 3489–3492.